



Metabolite profiles of human immunodeficiency virus infected CD4+ T cells and macrophages using LC–MS/MS analysis

Joseph A. Hollenbaugh^a, Joshua Munger^{a,b}, Baek Kim^{a,*}

^a Department of Microbiology and Immunology, University of Rochester Medical Center, Rochester, NY, USA

^b Department of Biochemistry and Biophysics, University of Rochester Medical Center, Rochester, NY, USA

ARTICLE INFO

Article history:

Received 17 February 2011

Returned to author for revision 12 April 2011

Accepted 16 April 2011

Available online 11 May 2011

Keywords:

HIV-1

Metabolism

CD4+ T cells

Macrophages

LC–MS/MS

ABSTRACT

Human immunodeficiency virus type 1 (HIV-1) infects both activated CD4+ T cells and macrophages. We tested if liquid chromatography–tandem mass spectrometry (LC–MS/MS) technology can monitor metabolic alterations induced by HIV-1 in the infected cells. Here we monitored glucose uptake and conducted LC–MS/MS-based metabolomic analysis in HIV-1 infected primary human CD4+ T cells and a macrophage model system: differentiated U1 (HIV-1 producing) and differentiated U937 (control) cells. HIV-1 infected CD4+ T cells have higher glucose uptake and increases in several metabolite pool sizes, whereas HIV-1 producing macrophages had substantial reductions in glucose uptake and steady state glycolytic intermediates. This data suggests that the two HIV-1 target cell types exhibit very different metabolic outcomes during viral production. This study also validates the LC–MS/MS technology as an effective metabolomic approach to monitor various metabolic alterations made by HIV-1 infection.

© 2011 Elsevier Inc. All rights reserved.

Background

Cellular metabolic pathways, such as glycolysis, tricarboxylic acid cycle (TCA cycle), lipid metabolism, amino acid and nucleotide synthesis, are targeted during viral infections to support the production of 1000 to 20,000 new viral progeny per infected cell (Chen et al., 2007; Horsfall, 1954). Recently studies show that human cytomegalovirus (HCMV) alters numerous aspects of host-cell metabolism, some of which were found to be critical for viral replication (Chambers et al., 2010; McArdle et al., 2011; Munger et al., 2008). Hepatitis virus type C infection has been shown to induce dysregulation of glucose utilization and lipid biosynthesis (Blackham et al., 2010; Herker et al., 2010; Mankouri et al., 2010). Many viruses, including poliovirus, Dengue, Epstein Barr virus and Human Immunodeficiency Virus type 1 (HIV-1), usurp the autophagy pathways, which are involved in sensing nutrient deprivation and energy stress, for the benefit of viral infection, immune evasion, and viral replication (Heaton and Randall, 2010; Shoji-Kawata and Levine, 2009).

HIV-1 causes acquired immune deficiency syndrome, and it uniquely infects both activated CD4+ T cells and terminally differentiated macrophages during the course of HIV-1 pathogenesis. While HIV-1 infection of CD4+ T cells induces G2 arrest and cell death within 2–3 days (Jowett et al., 1995), HIV-1 infection of macrophages leads to long-lived survival and low constitutive viral production,

generating viral reservoirs (Cosenza et al., 2004; Kilareski et al., 2009), which contribute to HIV-1 associated neurodegenerative diseases in the CNS (Cysique and Brew, 2009).

Collectively, it is becoming increasingly apparent that upon viral infection changes occur in the metabolic profile of the cell, which are critically important for viral replication. With this in mind, we sought to determine how HIV-1 impacts the cellular metabolic environments in activated CD4+ T cells and macrophages. Recent advances in metabolomic methodologies, such as LC–MS/MS technology, enable the simultaneous measurement of numerous cellular metabolic intermediates allowing for the elucidation of highly complex metabolic outcomes induced by viral infections at steady state level (Munger et al., 2006, 2008). Our previous HCMV findings indicate increased glucose uptake in HCMV-infected fibroblasts as compared to mock-infected cells. These data were further supported by increased steady state glycolytic and TCA-cycle metabolite pool sizes within the cells coupled with faster metabolite flux through glycolysis and TCA intermediates upon HCMV infection (Munger et al., 2008).

Due to the long-lived nature of HIV-producing macrophages, we hypothesized that the cellular metabolic landscape of HIV-infected macrophages could be different from that of HIV-infected CD4+ T cells, which were previously reported to robustly upregulate some cellular metabolic events (Chan et al., 2009). In addition, no metabolomic analysis on long-living, persistently infected cells has yet been reported. Therefore, in this study, we tested our hypothesis by monitoring the metabolic alterations that occur during viral production from primary CD4+ T cells and an HIV-1 infected human macrophage model system. Indeed, we find that the two HIV-1 target cell types have very different

* Corresponding author at: Department of Microbiology and Immunology, University of Rochester Medical Center, 601 Elmwood Avenue Box 672, Rochester, NY 14642, USA. Fax: +1 585 473 9573.

E-mail address: baek_kim@urmc.rochester.edu (B. Kim).

metabolic profiles. HIV-1 infected CD4+ T cells have significantly increased uptake of tritiated glucose, whereas infected macrophages have significantly reduced uptake of tritiated glucose. Using LC-MS/MS-based metabolomic analysis, we find that several steady state glycolytic intermediates are significantly upregulated in CD4+ T cells, whereas macrophages have significantly reduced level of several metabolites. Moreover, we find significant changes in several metabolites in the PPP, TCA cycle, and UDP-sugars for both cell types. We also examined NTP pools and found significant changes only for macrophages. Lastly, we examined ATP/ADP, NAD+/NADH and NADP+/NADPH ratios and found only macrophages have a significant change in the NADP+/NADPH ratio. Our LC-MS/MS data help provide a clearer understanding of cell type specific metabolic changes associated with HIV-1 viral replication.

Results and discussion

In this study, our goal is to test if the LC-MS/MS technology can monitor HIV-1 induced cellular metabolic alterations in CD4+ T cells and macrophages. To test this we compared HIV-1 infected versus non-infected primary human CD4+ T cells from the same donor (Fig. 1a). CD4+ T cells were infected with NLEGN-1 HIV-1 virus, which is the infectious HIV-1 NL4-3 strain that has all viral genes expressed in addition to GFP (Kutsch et al., 2002). CD4+ T cells were FACS-sorted into GFP+ (HIV-1 producing) and GFP- cells from the same donor, achieving 7–20% infection at the time of sorting. All CD4+ T cell experiments compared infected versus uninfected T cells at the same time for individual donors.

Due to the nature of macrophages being difficult to infect completely with HIV-1 and their tendency not to re-adhere once detached, we utilized a cell line model to mimic human HIV-1 infected macrophages (Fig. 1b). The human promonocytic U937 cells are the most commonly used HIV-1 monocyte/macrophage model system (Cassol et al., 2006). U1 cells are chronically HIV-1 infected U937 cells (Folks et al., 1987) and are widely used as a model system to study HIV-1 biology in macrophages (Bristow et al., 2008; Cassol et al., 2006; Fernandez Larrosa et al., 2008; Olivares et al., 2009; Spector and Zhou, 2008). U937 and U1 cells were differentiated into macrophages using Vitamin D3 and PMA treatment (Fig. 1b). U1 cells produced virus within 2 days as measured by intracellular expression and secreted p24 (Supplemental data 2a and b). In addition, U1 cells remained alive and have comparable cell death to U937 cells (Supplemental data 2c and d), indicating that HIV-1 production does not induce apoptosis for U1 cells, which is similar to what we observe with primary human macrophages.

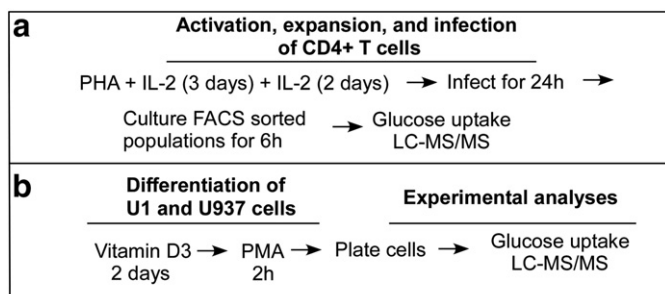


Fig. 1. Diagram of methods. a) Primary CD4+ T cells were expanded in culture in the presence of 5 µg/ml PHA and 10 ng/ml IL-2. After 5 days the cells were infected with NLEGN-1 HIV-1 virus for 24 h before FACS sorting the cells into GFP+ (HIV-1 producing cells) and GFP- (control) populations. The cells were allowed to recover for 6 h in DMEM media containing 10% FBS before being used for LC-MS/MS or glucose uptake assays. b) U1 and U937 cells were matured in the presence of 10 nM Vitamin D3 for two day prior to 100 nM PHA treatment for 1 h. Cells were then washed three times with media, counted and plated at 2 million cells/well. At day 2 of differentiation, macrophages were used for experiments.

A basic overview of metabolic pathways is illustrated in Fig. 2a showing the many different pathways that glucose can travel once entering the cell (Wamelink et al., 2008). First, we used tritiated 2-deoxyglucose (2-DOG) to monitor the cellular capacity for glucose uptake (Reusch et al., 1991). As shown in Fig. 2b and Supplemental data 3a, HIV-1 infected CD4+ T cells (GFP+) from three different human donors have a significant increase in 2-DOG uptake as compared to GFP- CD4+ T cells (control) from the same donor under the same culture conditions. In contrast, when we examined glucose uptake of the U937 and U1 macrophage model system, and observed that U1 macrophages have a significant reduction in 2-DOG uptake as compared to U937 macrophages (Fig. 1b and Supplemental data 3b). Since U1 and U937 cells have been passaged for many years, there may be additional, subtle changes that have occurred to both cell lines. However, both U1 and U937 cells have comparable 2-DOG uptake before differentiation (Supplemental data 3c), suggesting no predisposed gross changes in glucose uptake in latently infected U1 cells is observed. Overall, the absence of glucose uptake enhancement in U1 macrophages (HIV-1 producing) versus U937 macrophages implies that HIV-1 production does not induce additional glucose uptake during virus production. This finding is in contrast to our HIV-1 infected CD4+ T cell data (Fig. 2b) and the observations of another lytic viral infection (Munger et al., 2006, 2008).

Next we used LC-MS/MS to examine steady state levels of metabolic intermediates during viral infection. For HIV-1 infected CD4+ T cells and macrophage model system, a total of 66 metabolic small molecules were identified during steady state analysis (Supplemental Table 1: complete list). Our data for HIV-1 infected CD4+ T cells (analyzed as ratio of GFP+/GFP-) indicate that several glycolytic key metabolites: hexose-P, fructose 1,6-bisphosphate (FBP), glyceraldehyde-3P (G3P) and 3-phosphoglycerate (3PG) have significantly increased pool sizes by *T*-test analysis (Fig. 3a; shown as Log₂ converted data). This data together with the increased glucose uptake (Fig. 2b), suggests an increased rate of glycolysis for HIV-infected CD4+ T cells. These observations parallel previous findings in which increases in glycolytic metabolite concentrations correlated with increased glycolytic flux (Munger et al., 2006, 2008).

Next, we examined metabolic pools in macrophage model system (analyzed as the ratio of U1/U937) and found significant reductions in glycolytic intermediates: hexose-P, FBP and G3P (Fig. 3a). Coupled with the decrease in glucose uptake (Fig. 2b), these results suggest an HIV-induced suppression of glycolysis in macrophages. One surprising aspect of these data is the increase in pyruvate pool size despite the reduction of glucose uptake and decreased FBP levels. This could reflect either decreased pyruvate consumption by the TCA cycle in macrophages or perhaps increased pyruvate production from other carbon sources such as amino acid oxidation. Regardless, these data indicate that HIV-1 infection in CD4+ T cells and macrophages has very different metabolic outcomes.

Next, we examined metabolite pool sizes for the TCA cycle. As shown in Fig. 3b, aconitate and isocitrate are significantly increased for HIV-1 infected CD4+ T cells, while HIV-1 producing macrophages have a significantly larger malate pool. Collectively, the lack of detectable changes in multiple metabolite pool sizes suggests that the viral impact on the TCA cycle is not analogous to its impact on glycolysis. Ringrose et al. reported that several TCA cycle proteins are upregulated during late HIV-1 infection (Ringrose et al., 2008). While we do detect substantial changes to a few TCA metabolite pool sizes, we cannot clearly delineate this impact on the TCA cycle. Moreover, our data does not address HIV-modulation of TCA cycle flux or changes in metabolite pool sizes that feed into and out of the TCA cycle for other biosynthesis pathways. These data are in contrast to earlier findings for HCMV infection which showed increases in TCA cycle intermediates (Munger et al., 2006, 2008), suggesting that evolutionarily divergent viruses interact differently with the host-cell metabolic network. Alternatively, activation of glycolysis is sufficient

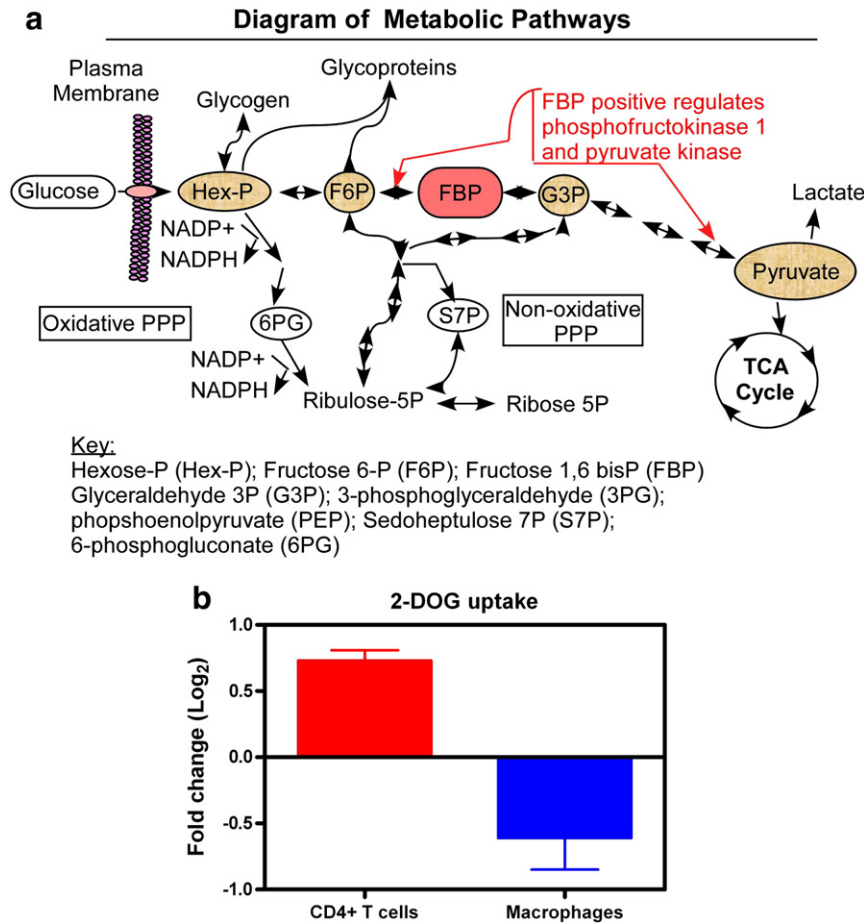


Fig. 2. Diagram of metabolic pathways. FBP is the major regulatory metabolite for glycolysis. It influences its own production and pyruvate, to stimulation of more glucose consumption. Pyruvate can be converted into lactate or further be processed to enter the TCA cycle. Alternative pathways of glucose use are the PPP, glycogen synthesis and glycosylation of proteins. The oxidative PPP is unidirectional and generates NADPH, whereas the non-oxidative PPP is reversible, allowing excess ribose to be converted into glycolytic intermediates or ribose generation from intermediates. **b)** Glucose uptake assay was performed as described in [Methods](#). Glucose uptake is shown for CD4+ T cells as the ratio of GFP+/GFP- (HIV-1+ positive/HIV-1 negative cells) and the ratio of U1/U937 macrophages (HIV-1 producing/control cells). Three independent experiments were done in triplicate for each cell type. Data displayed as Log₂ converted and SEM.

to support HIV-1 production in CD4+ T cells, while HCMV, having a larger DNA genome (230 kb) as compared to the small RNA genome (9.5 knt) of HIV-1, may require greater metabolic resources thus promoting the activation of both glycolysis and the TCA cycle.

Next we examined metabolite pool sizes. For the PPP, HIV-1 infected CD4+ T cells have a significant increase in sedoheptulose 7-P (S7P; non-oxidative PPP) and ribose-P, whereas macrophages have a significant decrease in 6-P-gluconate (6PG; oxidative PPP) and no significant change in S7P and ribose-P ([Fig. 4a](#)). These data suggest that infected CD4+ T cells may use the non-oxidative PPP to generate ribose at this late time point after infection. In addition, the PPP metabolite 6PG level is not significantly different (Log₂ = -0.09). These data are consistent with [Chan et al.](#); they showed no difference at the enzyme level for this metabolite at a late time point of infection ([Chan et al., 2009](#)). HIV-1 has an RNA genome; therefore we also examined nucleotide triphosphate (NTP) pool sizes in CD4+ T cells and macrophages. We recently reported that macrophages have a slightly lower NTP pools than activated PBMC, and the concentrations of pyrimidines are lower than purines ([Kennedy et al., 2010](#)). As shown in [Fig. 4b](#), no significant differences in NTP pool sizes were detected for CD4+ T cells. Yet for the macrophage model system, the pyrimidines: CTP and UTP pool sizes were significantly increased. We detected a decrease in GTP, yet this did not reach the level of significant difference using paired *T*-test.

We next examined the ATP/ADP, NAD+/NADH and NADP+/NADPH ratios ([Fig. 4c](#) and [Supplemental data 4](#)). For both cell populations, the ATP/ADP and NAD+/NADH ratios were not significantly different. These data supported our conclusion of very little change in the TCA cycle by HIV-1 infection. It has been well established for HIV-1 and other viruses that the redox levels: glutathione and NADPH, change within the infected cells ([Gu et al., 2001](#); [Jana and Pahan, 2004](#); [Korenaga et al., 2005](#); [Sagi and Fluhr, 2001](#)). The NADP+/NADPH ratio for macrophages was significantly different, but not for CD4+ T cells ([Fig. 4c](#)). This data and the 6PG PPP metabolite data suggest an overall reduction in the ability to generate NADPH. Furthermore, these data suggest that HIV-1 producing U1 macrophages may be compromised in their ability to generate de novo nucleotides and fatty acids. This can be addressed in future studies using more tradition biochemical assays.

Finally, we examined the UDP-sugar pools within the different cell types. UDP-sugars are metabolic intermediates used in glycosylation of proteins. HIV-1 gp120 and gp41 proteins are highly glycosylated, are key targets for antibody binding to prevent infection, and are critical for HIV-1 pathogenesis ([Montefiori et al., 1988](#); [Pal et al., 1989](#); [Raska et al., 2010](#)). We detect a significant increase in UDP-glucose pool size for CD4+ T cells ([Fig. 4d](#)). UDP-D-glucuronate pool size was not significantly changed in either CD4+ T cells or macrophages. UDP-N-acetyl-glucosamine pool size was significantly increased in both CD4+ T cells and macrophages, whereas N-acetyl-glucosamine-

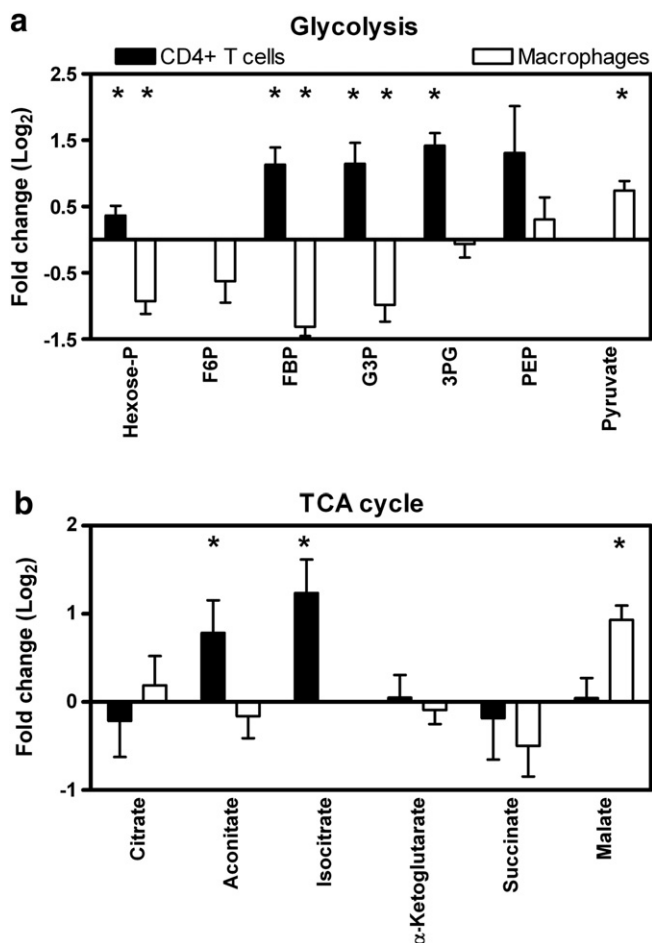


Fig. 3. LC-MS/MS analysis of glycolysis and TCA cycle metabolic pools. **a)** LC-MS/MS analysis of glycolytic intermediates for CD4+ T cells (solid) and macrophages (open) are shown as fold change in data. Metabolites that have a significant difference are denoted with asterisks. **b)** TCA cycle intermediate pool sizes are compared as described above. For CD4+ T cells, the ratio of GFP+/GFP– metabolite intensities was compared, whereas the ratio of U1/U937 metabolite intensities is shown for macrophages. Significant differences were determined using paired *T*-test. For CD4+ T cells, four independent donors were done in duplicate ($n=8$). Seven LC-MS/MS runs were compared for U1 and U937 cells. Data displayed as Log₂ converted and SEM.

1P was significantly increased in macrophages only (Fig. 4d). These data indicate that UDP-sugar pathways may be potential targets for metabolic chemical inhibitors, since they are increased in both cell types. Future experiments will need to be done in order to confirm that reducing UDP-sugar synthesis has an effect on HIV-1 viral replication.

Clearly our data indicates that LC-MS/MS technology is attractive when measurement of multiple metabolic intermediates is desired. Our strongest data using LC-MS/MS comes from the analysis of glycolytic intermediates (Fig. 3a), which will require additional future studies to examine both RNA and protein levels under these conditions. The limitations of these results are 1) the relative low detection sensitivity presumably due to the limited biomass sizes, compared to the previous HCMV data, particularly in PPP and TCA pathways (Munger et al., 2006, 2008), 2) the potential delay of sample preparation for suspension cells, which requires centrifugation before lysis, which may be problematic for metabolic kinetic readouts (i.e. flux analysis), as compared to adherent cells which can be directly methanol lysed on the plates, and finally, 3) the difficult nature of primary human macrophage infection from donor to donor. These

technical limitations partially attribute cell types used during this study, and require further work.

Conclusion

Our data suggests that the two HIV-1 target cell types exhibit very different metabolic outcomes during viral production, and this study also validates the LC-MS/MS technology as an effective metabolomic approach to monitor various metabolic alterations made by HIV-1 infection.

Materials and methods

Cells

The U937 cell line was purchased from the American Type Culture Collection, whereas the U1 cell line was acquired through the NIH AIDS Research and Reference Program. Both cell lines were grown in RPMI 1640 media supplemented with 10% FBS and penicillin and streptomycin antibiotics (complete media). Cells were split 1:5 dilution and treated with 10 nM Vitamin D3 (Sigma) at day –2. At day –1, media was doubled and supplemented with Vitamin D3. At day 0, cells were transferred to 50 ml tubes and treated with 100 nM PMA for 2 h. Cells were washed three times with PBS, resuspended in 10 ml of complete media and counted. Two million cells per well were plated in 6-well plate with a final volume of 4 ml/well of RPMI 1640 media with 10% FBS. After 2 days of differentiation, U937 and U1 cells were used for experiments.

Primary human CD4+ T cells were positively selected for using MACS isolation from buffy coats (New York Blood Services, Long Island, NY). Cells were at 10 million cells/ml stored at –80 °C before use. For CD4+ T cells activation, 60–120 million cells were thawed and placed in media. Cells were centrifuged at 1200 rpm for 7 min. The pellet was resuspended in 15 ml of DMEM media containing 5% FBS/30 million cells. The cell suspension was placed in a T75 flask and 5 µg/ml of PHA (Sigma) and 10 ng/ml IL-2 (Roche; NIH AIDS Research and Reference Reagents) were added. At day 2, 7.5 ml DMEM media and 10 ng/ml IL-2 were added. At day 3, cells were centrifuged at 1200 × g rpm for 7 min. Two T75 flasks were combined and pellets resuspended in 40 ml of DMEM media with 10 ng/ml IL-2. Cells were allowed to expand for two more days. At day 5, cells were harvested at 1200 rpm for 7 min. Cells were resuspended in 10 ml of media and counted.

HIV-1 virus generation

pNLEG-1 was a kind gift from Dr. Levy (Kutsch et al., 2002). Plasmid was transfected into Stable 2 *Escherichia coli* strain and then Qaigen Maxi preparation was done. 292FT cells (Invitrogen) grown in T225 flasks were transfected with 60 µg pNLEG-1 and 10 µg pVSV-g plasmids using 140 µl polyethylenimine (1 mg/ml) in 37 ml DMEM media/flask. Day 1 HIV-1 production was discarded and fresh DMEM media + 0.1% DMSO were added. At day 2, media was harvested and replaced with fresh DMEM media + 0.1% DMSO. The media was centrifuged at 3500 rpm for 7 min to remove cellular debris. Media was stored at 4 °C in T75 flask. Day 2 media was harvested and processed as day 1. Both days of collection were pooled and FBS was added to 5% volume. In addition, 10 ng/ml IL-2 was added to the T75 flask. This large cocktail was then used to infect the primary activated CD4+ T cells.

CD4+ T cell infection

Ten million activated CD4+ T cells were placed in 15 ml of HIV-1 media (TPP petri dishes). Dishes were placed on an orbital shaker for 24 h in the incubator. We found that this led to the fastest increase in GFP+ cells. Cells were then harvested from the dishes and centrifuged.

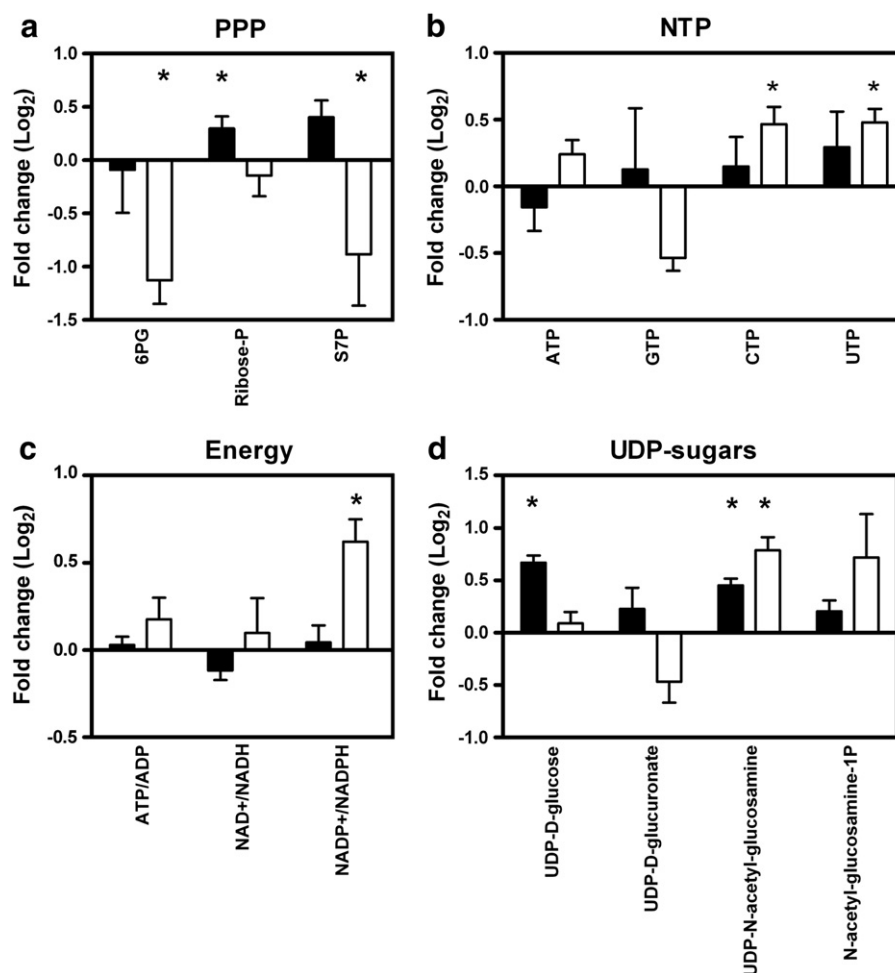


Fig. 4. LC-MS/MS analysis of metabolites used in viral production. a) PPP pathway was examined for CD4+ T cells (solid) and macrophages (open). Significantly different metabolites are indicated by asterisks. b) NTP pools were examined and found to change more for macrophages than T cells. c) The ATP/ADP, NAD+/NADPH and NADP+/NADPH ratios were examined for the different cell types. d) Sugar derivative pool sizes were examined using LC-MS/MS analysis. Data sets are stated and plotted as indicated in Fig. 3 legend.

Pellets were resuspended in 2 ml of DMEM media and filtered into FACS tubes. Additional media was added to adjust cells/ml to under 50 million before sorting.

FACS sorting

The University of Rochester has a FACS Core Facility. Cells were FACS Sorted using BD FACS Aria IIu machine, which is in a BioProtect III hood (The Baker Co.) using BSL-2+ conditions. Single T cells were discriminated using FSC and SSC parameters before sorting GFP+ (HIV-1+) and GFP- (HIV-1 negative) populations. The gating profile from the FACS sorter is shown in [Supplemental data 1](#) and shown a very tight gate GFP- cells and a liberal collection gate for GFP+ cells. We had between 7 and 20% GFP+ populations for the seven different donors. This determined as to which type of experiment was done after sorting. We needed 3 million cells/tube for LC-MS/MS, whereas the glucose uptake assay had 1.5–2 million cells/tube. CD4+ T cells were analyzed in duplicate for LC-MS/MS analysis, whereas triplicate samples for each of the GFP+ and GFP- populations were analyzed for the glucose uptake assay.

Liquid chromatography–tandem mass spectrometry (LC-MS/MS)

For U1 and U937 cells steady state analysis, media was removed from day 2 differentiated cells and replaced with serum-free DMEM

media lacking sodium pyruvate. After 1 h at 37 °C, the media was aspirated and dry ice cold 80% methanol was added. Samples were stored at –80 °C for 5 min followed by processing with a rubber policeman to remove attached cells. Supernatant was transferred to a 15 ml conical tube and vortexed for 1 min. Samples were centrifuged at 3500 rpm for 5 min. The supernatant was transferred to a new tube. Pellets were washed with 1 ml of dry ice cold 80% methanol. Samples were centrifuged and supernatants consolidated for each sample. Samples were dried under nitrogen gas. Once dried, samples were stored at –80 °C until analysis.

For FACS Sorted CD4+ T cells, 3×10^6 cells were placed in cryovials with DMEM containing 10% dialyzed FBS serum. Cells were allowed to recover for 6 h in the tissue culture incubator. After recovery time, each sample was centrifuged at 4 K rpm for 10 s. Supernatant was removed using vacuum and 1 ml of dry ice cold 80% methanol was added. Tubes were vortexed for 1 min, and then centrifuged at 15 K rpm for 1 min. Supernatant was removed and placed in a 15 ml tube. Cell pellet was washed with 0.5 ml dry ice cold 80% methanol. Tubes were centrifuged again and supernatants pooled. Supernatants were dried using nitrogen gas. Once dried, samples were stored at –80 °C until analysis.

Samples were removed from the –80 °C and allowed to equilibrate to room temperature. The cell pellet was resuspended in 100 μ l 50% methanol and liquid transferred to 1.5 ml centrifuge tube. Cellular debris was removed by 15 K rpm centrifugation for 10 min and 75 μ l of supernatant was transferred to a LC-MS/MS vial and

capped. Ten microliters of sample was autoloading into LC-20 AD HPLC system (Shimadzu) for metabolite separation. The LC was coupled to a mass spectrometer running in negative mode with an ESI source using reversed phase chromatography with an amine-based ion pairing agent. A Synergi Hydro-RP column (150 by 2 mm with a 5- μ m particle size; Phenomenex) was used with the following LC parameters: autosampler temperature, 4 °C; column temperature, 40 °C; flow rate, and 200 μ l/min. The LC solvents were as follows: solvent A, 100% methanol; solvent B, 10 mM tributylamine and 15 mM acetic acid in 97:3 water-methanol. The HPLC gradients were as follows: for $t=0$, 100% B; for $t=5$, 100% B; for $t=10$, 80% B; for $t=20$, 80% B; for $t=35$, 35% B; for $t=38$, 5% B; for $t=42$, 5% B; for $t=43$, 100% B; and for $t=50$, 100% B. Mass spectrometric analyses were performed with a TSQ Quantum Ultra triple-quadrupole mass spectrometer (Thermo Fisher Scientific) with mass spectrometry parameters as per Bajad et al. (2006).

Data analysis and graphing

MS data were acquired using Xcalibur software (Thermo Fisher Scientific). Each metabolite measurement was in the form of a selected reaction monitoring scan event (SRM) occurring at a specific HPLC retention time. Each SRM consists of: a metabolite specific parent ion m/z , a collision cell energy, and a metabolite-specific product ion resulting from collision with argon gas in the collision cell. Metabolite retention times and SRMs were previously empirically determined using pure chemical standards and have formerly been reported (Bajad et al., 2006). The resulting data were exported into mzRock free shareware (<http://code.google.com/p/mzrock/>), which allows automated analysis of targeted metabolomics data. To quantify metabolite levels, peak heights for different metabolite SRMs were determined for each sample. A metabolite was not analyzed further if: (i) its signal for all viral and mock samples was undetectable; (ii) its maximum signal for all viral or mock samples was less than 2-fold that of the maximum signal in the methanol control sample; or (iii) the observed signal likely resulted from a naturally occurring heavy isotope of another metabolite. Data from each donor set was compared pair wise as they were run and paired T-test used to evaluate significant differences. Data was plotted with standard error of mean (SEM) using Prism software (GraphPad Software).

2-DOG uptake assay

For U1 or U937 cells, 1×10^6 cells/well were differentiated in 12-well plates. At day 2 of differentiation, media was removed and cells cultured for 2 h under serum free conditions. After incubation, media was replaced with 0.5 ml DMEM media (glucose free) containing 1.0 μ Ci 2-DOG/ml. Cells were cultured for 10 min at 37 °C. Preliminary assays were done with macrophage and 293FT cells and found that 2-DOG uptake was still in the linear range even after 30 min of incubation (data not shown). Afterwards, the plates were placed on ice, media removed, cells washed thrice with ice cold PBS. Cells were lysed using ELB buffer with 0.1% SDS for 20 min at 37 °C. Scintillation counts were collected using 0.4 ml. Data was normalized to total protein (BioRad protein assay). Samples were done in triplicate.

For CD4+ T cells, $1.5\text{--}2 \times 10^6$ cells were placed in cryovials with complete DMEM media after FACS sorting. The cells were allowed to recover for 6 h. The vials were then closed and centrifuged at 4 K rpm for 10 s. The media was removed by aspiration, and 0.5 ml DMEM media (glucose free) containing 1.0 μ Ci 2-DOG/ml was added. The cells were incubated at 37 °C for 10 min, before being centrifuged at 4 K rpm for 15 s. Media was carefully removed and cell pellet washed once with ice cold PBS. After centrifugation, the pellet was lysed using ELB buffer with 0.1% SDS for 20 min at 37 °C. Scintillation counts were collected using 0.4 ml. Data was normalized to total protein. Samples were done in triplicate for three independent donors.

Supplementary materials related to this article can be found online at doi:10.1016/j.virol.2011.04.007.

Competing interests

The authors declare that they have no competing interests.

Authors' contributions

JAH performed experiments. JAH, JM and BK reviewed the data and wrote the manuscript.

Acknowledgments

This study was supported by NIH grants: R01AI081773 (JM), T32 DA07232 (JAH), and A1077401 (BK). We would like to thank the Rochester FACS Core for the sorting and AIDS Research and Reference Reagent Program for reagents. We would like to thank Edward Kennedy and Erin Noble for reading and comments on this manuscript.

References

- Bajad, S.U., Lu, W., Kimball, E.H., Yuan, J., Peterson, C., Rabinowitz, J.D., 2006. Separation and quantitation of water soluble cellular metabolites by hydrophilic interaction chromatography–tandem mass spectrometry. *J. Chromatogr. A* 1125 (1), 76–88.
- Blackham, S., Baillie, A., Al-Hababi, F., Remlinger, K., You, S., Hamatake, R., McGarvey, M.J., 2010. Gene expression profiling indicates the roles of host oxidative stress, apoptosis, lipid metabolism, and intracellular transport genes in the replication of hepatitis C virus. *J. Virol.* 84 (10), 5404–5414.
- Bristow, C.L., Wolkowicz, R., Trucy, M., Franklin, A., Di Meo, F., Kozlowski, M.T., Winston, R., Arnold, R.R., 2008. NF-kappaB signaling, elastase localization, and phagocytosis differ in HIV-1 permissive and nonpermissive U937 clones. *J. Immunol.* 180 (1), 492–499.
- Cassol, E., Alfano, M., Biswas, P., Poli, G., 2006. Monocyte-derived macrophages and myeloid cell lines as targets of HIV-1 replication and persistence. *J. Leukoc. Biol.* 80 (5), 1018–1030.
- Chambers, J.W., Maguire, T.G., Alwine, J.C., 2010. Glutamine metabolism is essential for human cytomegalovirus infection. *J. Virol.* 84 (4), 1867–1873.
- Chan, E.Y., Sutton, J.N., Jacobs, J.M., Bondarenko, A., Smith, R.D., Katze, M.G., 2009. Dynamic host energetics and cytoskeletal proteomes in human immunodeficiency virus type 1-infected human primary CD4 cells: analysis by multiplexed label-free mass spectrometry. *J. Virol.* 83 (18), 9283–9295.
- Chen, H.Y., Di Mascio, M., Perelson, A.S., Ho, D.D., Zhang, L., 2007. Determination of virus burst size in vivo using a single-cycle SIV in rhesus macaques. *Proc. Natl. Acad. Sci. U. S. A.* 104 (48), 19079–19084.
- Cosenza, M.A., Zhao, M.L., Lee, S.C., 2004. HIV-1 expression protects macrophages and microglia from apoptotic death. *Neuropathol. Appl. Neurobiol.* 30 (5), 478–490.
- Cysique, L.A., Brew, B.J., 2009. Neuropsychological functioning and antiretroviral treatment in HIV/AIDS: a review. *Neuropsychol. Rev.* 19 (2), 169–185.
- Fernandez Larrosa, P.N., Croci, D.O., Riva, D.A., Bibini, M., Luzzi, R., Saracco, M., Mersich, S.E., Rabinovich, G.A., Martinez Peralta, L., 2008. Apoptosis resistance in HIV-1 persistently-infected cells is independent of active viral replication and involves modulation of the apoptotic mitochondrial pathway. *Retrovirology* 5, 19.
- Folks, T.M., Justement, J., Kinter, A., Dinarello, C.A., Fauci, A.S., 1987. Cytokine-induced expression of HIV-1 in a chronically infected promonocyte cell line. *Science* 238 (4828), 800–802.
- Gu, Y., Wu, R.F., Xu, Y.C., Flores, S.C., Terada, L.S., 2001. HIV Tat activates c-Jun amino-terminal kinase through an oxidant-dependent mechanism. *Virology* 286 (1), 62–71.
- Heaton, N.S., Randall, G., 2010. Dengue virus-induced autophagy regulates lipid metabolism. *Cell Host Microbe* 8 (5), 422–432.
- Herker, E., Harris, C., Hernandez, C., Carpentier, A., Kaehlcke, K., Rosenberg, A.R., Farese Jr., R.V., Ott, M., 2010. Efficient hepatitis C virus particle formation requires diacylglycerol acyltransferase-1. *Nat. Med.* 16 (11), 1295–1298.
- Horsfall Jr., F.L., 1954. On the reproduction of influenza virus; quantitative studies with procedures which enumerate infective and hemagglutinating virus particles. *J. Exp. Med.* 100 (2), 135–161.
- Jana, A., Pahan, K., 2004. Human immunodeficiency virus type 1 gp120 induces apoptosis in human primary neurons through redox-regulated activation of neutral sphingomyelinase. *J. Neurosci.* 24 (43), 9531–9540.
- Jowett, J.B., Planelles, V., Poon, B., Shah, N.P., Chen, M.L., Chen, I.S., 1995. The human immunodeficiency virus type 1 vpr gene arrests infected T cells in the G2+M phase of the cell cycle. *J. Virol.* 69 (10), 6304–6313.
- Kennedy, E.M., Gavegnano, C., Nguyen, L., Slater, R., Lucas, A., Fromentin, E., Schinazi, R.F., Kim, B., 2010. rNTPs as substrate of human immunodeficiency virus type 1 reverse transcriptase in human macrophages. *J. Biol. Chem.* 285 (50), 39380–39391.
- Kilareski, E.M., Shah, S., Nonnemacher, M.R., Wigdahl, B., 2009. Regulation of HIV-1 transcription in cells of the monocyte-macrophage lineage. *Retrovirology* 6, 118.

- Korenaga, M., Wang, T., Li, Y., Showalter, L.A., Chan, T., Sun, J., Weinman, S.A., 2005. Hepatitis C virus core protein inhibits mitochondrial electron transport and increases reactive oxygen species (ROS) production. *J. Biol. Chem.* 280 (45), 37481–37488.
- Kutsch, O., Benveniste, E.N., Shaw, G.M., Levy, D.N., 2002. Direct and quantitative single-cell analysis of human immunodeficiency virus type 1 reactivation from latency. *J. Virol.* 76 (17), 8776–8786.
- Mankouri, J., Tedbury, P.R., Gretton, S., Hughes, M.E., Griffin, S.D., Dallas, M.L., Green, K.A., Hardie, D.G., Peers, C., Harris, M., 2010. Enhanced hepatitis C virus genome replication and lipid accumulation mediated by inhibition of AMP-activated protein kinase. *Proc. Natl. Acad. Sci. U. S. A.* 107 (25), 11549–11554.
- McArdle, J., Schafer, X.L., Munger, J., 2011. Inhibition of Calmodulin-dependent kinase kinase (CaMKK) blocks Human Cytomegalovirus-induced glycolytic activation and severely attenuates production of viral progeny. *J. Virol.* 85 (2), 705–714.
- Montefiori, D.C., Robinson Jr., W.E., Mitchell, W.M., 1988. Role of protein N-glycosylation in pathogenesis of human immunodeficiency virus type 1. *Proc. Natl. Acad. Sci. U. S. A.* 85 (23), 9248–9252.
- Munger, J., Bajad, S.U., Collier, H.A., Shenk, T., Rabinowitz, J.D., 2006. Dynamics of the cellular metabolome during human cytomegalovirus infection. *PLoS Pathog.* 2 (12), e132.
- Munger, J., Bennett, B.D., Parikh, A., Feng, X.J., McArdle, J., Rabitz, H.A., Shenk, T., Rabinowitz, J.D., 2008. Systems-level metabolic flux profiling identifies fatty acid synthesis as a target for antiviral therapy. *Nat. Biotechnol.* 26 (10), 1179–1186.
- Olivares, I., Ballester, A., Lombardia, L., Dominguez, O., Lopez-Galindez, C., 2009. Human immunodeficiency virus type 1 chronic infection is associated with different gene expression in MT-4, H9 and U937 cell lines. *Virus Res.* 139 (1), 22–31.
- Pal, R., Hoke, G.M., Sarngadharan, M.G., 1989. Role of oligosaccharides in the processing and maturation of envelope glycoproteins of human immunodeficiency virus type 1. *Proc. Natl. Acad. Sci. U. S. A.* 86 (9), 3384–3388.
- Raska, M., Takahashi, K., Cernekova, L., Zachova, K., Hall, S., Moldoveanu, Z., Elliott, M.C., Wilson, L., Brown, R., Jancova, D., Barnes, S., Vrbkova, J., Tomana, M., Smith, P.D., Mestecky, J., Renfrow, M.B., Novak, J., 2010. Glycosylation patterns of HIV-1 gp120 depend on the type of expressing cells and affect antibody recognition. *J. Biol. Chem.* 285 (27), 20860–20869.
- Reusch, J.E., Begum, N., Sussman, K.E., Draznin, B., 1991. Regulation of GLUT-4 phosphorylation by intracellular calcium in adipocytes. *Endocrinology* 129 (6), 3269–3273.
- Ringrose, J.H., Jeeninga, R.E., Berkhout, B., Speijer, D., 2008. Proteomic studies reveal coordinated changes in T-cell expression patterns upon infection with human immunodeficiency virus type 1. *J. Virol.* 82 (9), 4320–4330.
- Sagi, M., Fluhr, R., 2001. Superoxide production by plant homologues of the gp91(phox) NADPH oxidase. Modulation of activity by calcium and by tobacco mosaic virus infection. *Plant Physiol.* 126 (3), 1281–1290.
- Shoji-Kawata, S., Levine, B., 2009. Autophagy, antiviral immunity, and viral counter-measures. *Biochim. Biophys. Acta* 1793 (9), 1478–1484.
- Spector, S.A., Zhou, D., 2008. Autophagy: an overlooked mechanism of HIV-1 pathogenesis and neuroAIDS? *Autophagy* 4 (5), 704–706.
- Wamelink, M.M., Struys, E.A., Jakobs, C., 2008. The biochemistry, metabolism and inherited defects of the pentose phosphate pathway: a review. *J. Inher. Metab. Dis.* 31 (6), 703–717.